Temperature Measurement Method by Infrared Radiation Pyrometer Using Chopped Broadband Radiation - Signal Conditioning and Acquisition Elements Design

K. T. Aminu, D. D. Yakubu, S.A. Baraza, B. D. Halilu

Department of Electrical Engineering

Abubakar Tatari Ali Polytechnic Bauchi

Nigeria

_____

ABSTRACT

In this paper, we report the design of a signal conditioning and acquisition elements of a chopped broadband radiation pyrometer for measuring temperature in the range of 900 ^{0} C to 1200 ^{0} C. We also report the selection of a suitable chopping frequency within the physical properties of the system and provided the calibration characteristics for the pyrometer. Based on the results, it was found that the designed signal conditioning circuit was able to produce an output voltage of 0.24 – 0.60 V corresponding to the temperature measuring range of the pyrometer. This was achieved through the use of a phase-sensitive detector (PSD) in the form of a lock-in amplifier in combination with a low pass filter. A suitable chopping frequency of 30 Hz was chosen for the shutter pulse so that the detector can have sufficient time to settle before the next shutter pulse transition. Finally, the result also shows that the calibration characteristic of the pyrometer presumes an approximately linear relationship.

Keywords: Contactless temperature sensor, Pyrometer, Infrared, Chopped Broadband, Signal Conditioning, Detector, Lock-In Amplifier.

_____

1. INTRODUCTION

High temperature measurements of objects are needed in many technical and research applications. For technical applications, however, the pyrometer should be simple, low cost, easy to handle and suitable for temperature measurements with reasonable accuracy. The primary focus of the present study is the design of signal conditioning circuit and acquisition elements for a non-contact temperature measurement of objects using chopped broadband radiation pyrometer. In recent years, the chopped broadband radiation pyrometer has been used for high temperature measurements because of its unique feature. This feature is a mechanical shutter that closes and opens the gate to the detector intermittently to prevent it from being burnt due to high temperature [1-2]. However, there are other techniques of high temperature measurement currently in use: narrow band radiation pyrometer and the broadband (unchopped) radiation pyrometer [3]. All these systems of temperature measurement operate on the same principle. However, in contrast, the chopped broadband radiation pyrometer differs from the traditional systems only because of the peculiar feature [1]. The errors of temperature measurements using classic approaches are often relatively high and it is very difficult to estimate such errors. These errors are due to the actual surface condition of the object, the effect of oxidation and the coating of the black body [2] [4]. The main purpose of the broadband radiation pyrometers is that they can potentially bring significant improvement in accuracy in non-contact temperature measurements, particularly in the case of so called difficult objects. These objects are considered to be the ones whose emissivity depends on the wavelength and time. Such cases can be found in many technical applications, and particularly often in the steel and semiconductor industry [4]. Additionally, the measurement accuracy of the system can be increased by reducing the influence of background temperature of the optical system. Hence, the need for conditioning the information acquired [2]. In recent years, there has been an increasing amount of literature on infrared pyrometer temperature measurement system [2] [4-8].

A brief background of infrared systems for non-contact temperature measurement, using the radiation emitted by the object under test, is presented in Section 1. The basic theory of the radiation pyrometer and the detector is presented in Section 2. The design details are presented in Section 3. Results obtained using the design parameters are given in section 4, and conclusions are drawn in Section 5.

2. THEORY

A. Basic Theory

All bodies emit electromagnetic radiation as a function of their temperature above absolute zero. The ideal emitter is termed a black body: from Planck's law, the spectral existence of radiation emitted by a black at a temperature T K is [5]:

$$W^{BB}(\lambda, T) = \frac{C_1}{\lambda^5 \left[exp \left(\frac{C_2}{\lambda T} \right) - 1 \right]} \qquad (1)$$

where $W^{BB}(T, \lambda)$ is the hemispherical spectral radiant intensity C_1 and C_2 are Plank's constants with values of $37,413 \text{W} \mu\text{m}^4/\text{cm}^2$ and $14,388 \mu\text{m}$ K respectively, λ is the wavelength of radiation in μm, and T the absolute temperature of the blackbody in degree Kelvin. However, the Wien's approximation is given by [5]:

$$W^{BB}(\lambda, T) = \frac{C_1}{\lambda^5 exp \left(C_2 / \lambda T \right)} \qquad (2)$$

can be used with an error of 10 % for values of $\lambda T < 3125 \mu\text{m}$ K. A correlation for the maximum of the spectral radiation energy can be derived from Equation (1), which is called the Wien's displacement law:

$$\lambda_{max} T = 2897.8 \, \mu m \, K \qquad (3)$$

However, in some cases, the influence of emissivity variations can be reduced tremendously by the use of two-color fiber-optic pyrometers measuring the emitted radiation at two specific wavelength bands [5].

i. Spectral radiation pyrometer

An equation for the total rate of radiation emitted per second is given by [4] [9]:

$$P_D = KT^4 \, (Wm^{-2}K^4) \qquad (4)$$

where T is the absolute temperature of the body and K is a constant of radiation that depends on the heat intensity, the nature of the heat spectrum and the kind of material of the body. For this application K is taken as 50 for the detector material. The power spectral density of this emission varies with temperature in the manner shown below. The major part of the frequency spectrum lies within the band of wavelengths between 0.3 μm and 40 μm, which corresponds to the visible and infrared ranges. As the magnitude of the variation varies with the temperature, measurement of the emission from a body allows the temperature to be calculated. Choice of the best method of measuring the emitted radiation depends on the temperature of the body. At low temperatures, the peak of the power spectral density function lies in the infrared region, whereas at higher temperatures it moves towards the visible part of the spectrum. This phenomenon is observed as the red glow which a body begins to emit as its temperature is increased beyond 600 ^{o}C [9].
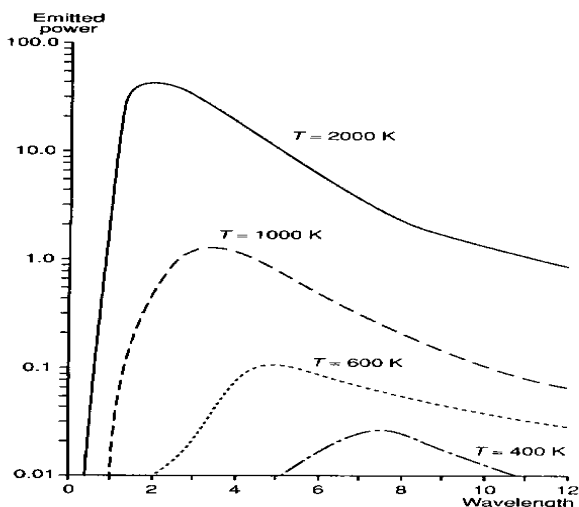

Figure 1: Radiation spectrum of an object heated at different temperature [9]

ii. Pyrometer

All the alternative forms of radiation pyrometer have an optical system which is similar to that in the optical pyrometer and focuses the energy emitted from the measured body. They differ, however, by omitting the filament and eyepiece and using instead an energy detector in the same focal plane as the eyepiece was. The radiation detector is either a thermal detector, which measures the temperature rise in a black body at the focal point of the optical system or a photon detector. Thermal detectors respond equally to all wavelengths in the frequency spectrum whereas photon detectors respond selectively to particular band within the full spectrum [9].

Radiation thermometers have one advantage in that they do not require being in contact with the hot body in order to measure its temperature. Thus, there is no disturbance at all in the measured system. Furthermore, there is no possibility of contamination, which is particularly important in the food industries and other process industries. They are also capable of measuring the temperature of moving bodies, for instance the temperature of steel bars in rolling mill [7] [9].

iii.   The chopped broad- band radiation pyrometer

A number advantages accrue when the radiation coming from the target to the detector is interrupted periodically (chopped) at a fixed frequency; therefore many infrared systems employ this technique. When high sensitivity is needed, amplification is required, and high gain ac amplifiers are easier to construct than their dc counterparts. This is usually the main reason for using choppers. Additional benefits related to ambient- temperature compensation and reference-source comparison also may be obtained. Systems employing thermal (broadband) and photon (restricted-band) detectors and choppers are in common use. Here in this application special consideration is given to thermal detectors [9].

iv.   Thermal detectors

Thermal detectors are blackened elements designed to absorb a maximum of the incoming radiation at all wavelengths. The absorbed radiation causes the temperature of the detector to rise until equilibrium is reached with heat losses to the surroundings. In order to examine the factors affecting both the sensitivity and time constant of a thermal detector, we now calculate the transfer function relating detector temperature T_D to power P_D [4][9]. The heat balance equation for the detector is:

$$P_D - UA(T_D - T_S) = MC\frac{dT_D}{dt} \qquad (5)$$

where T_D is the total incident power on the detector, T_S is the surrounding temperature, M detector mass in kg, C detector specific heat in J kg^{-1} ^{o}C^{-1}, A detector surface area in m^2 , and U represents the heat transfer coefficient in W m^{-2} ^{o}C^{-1}.

Rearranging Equation (5), we have:

$$T_D + \tau\frac{dT_D}{dt} = {P_D}/{UA} + T_s \qquad (6)$$

where time constant $\tau = \frac{MC}{UA}$. To obtain steady state solution, we set $\frac{dT_D}{dt} = 0$,

$$T_D = {P_D}/{UA} + T_S \qquad (7)$$

This result is intuitively reasonable since it says that T_D is proportional to P_D, the rate of heat influx and inversely proportional to UA, which governs the rate of heat loss [9].

3. PYROMETER SYSTEM DESIGN

A block diagram of the pyrometer system design is illustrated in Figure 2. It includes the radiation source (hot object whose temperature is to be measured), the optical filter, and the radiation/photodetector with corresponding lock-in amplifier and low pass filter, thus performing the signal conditioning. The active element close to the measuring unit corresponds to the optic filter. It is mechanically powered by the rotating shutter and driven by an electrical square signal to perform an on/off control. The mechanical rotating shutter is for switching of the chopped spectral bands simultaneously.
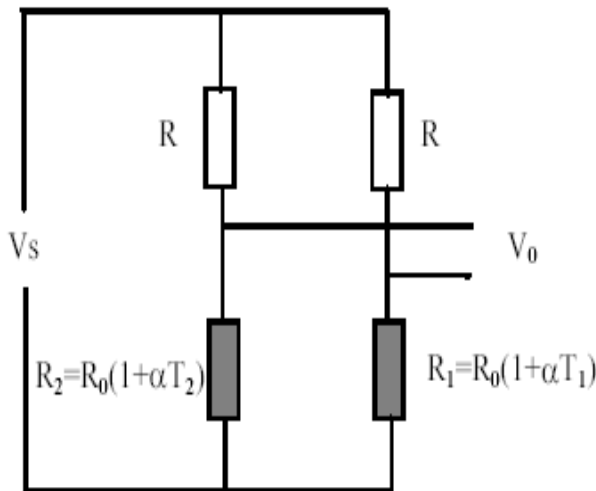
Figure 2: Schematic of the pyrometer system design with mechanically powered rotating shutter

The signal processing system (Figure 2) is designed to be able to modulate the optical signal (on/off control) and to demodulate the radiation emitted by the hot object so as to significantly reduce the effect of environmental noise. The photodetector with high-gain transimpedance amplifier is used to convert the receiving light from radiation to an output voltage. The optical filter is placed close to the hot object and before the photodetector to minimise the influence of atmospheric absorption on a signal from the object to the detector. The detector absorbs radiation whose wavelength is shorter than the cut-off wavelength. Absorption of such radiation causes an increase in electrical conductivity of the material and corresponding decrease in the detector resistance. This effect enables the system to measure radiation reaching the detector [8].

Information about the radiation signals measured in the system from the PSD (lock-in amplifier + low pass filter) through the data acquisition (DAQ) system to personal computer (PC). A software application is usually developed to control the communication process between the DAQ and the PC, to carry out calculations, calibration, and visualisation of the measurement results.

i. Mechanical Rotating Shutter Design

The total radiation released per unit surface area of a black body is given according to the Stefan-Boltzman law as given in Equation (4). The time constant and chopping frequency of the thermal detector governs the speed of the mechanical rotating shutter. The time constant is given by:

$$\tau = \frac{MC}{UA} \tag{8}$$

The chopping frequency of the rotating shutter is also given by:

$$f_c = \frac{1}{2\pi\tau} \tag{9}$$

ii. The Thermal Detector Design

The bolometer is commonest form of thermal detectors and it is the kind used in this application. It is a metal or semiconductor (thermistor) resistance material in the form of films or flakes which are blackened to maximize the absorption of the incoming radiation. The incident power P_D (W) would heat the detector to a temperature T_D (°C) which is usually above the surrounding temperature T_S (°C) [1]. The heat balance equation for the detector is given by Equation (5). By equation (7), a relationship has been established that gives the intercept as T_S and the gradient as the inverse of the product UA when presented graphically.

Since the bolometer is a passive resistive device, a bridge circuit can be used to produce an output voltage proportional to temperature. Two sensors, labeled R_1 and R_2 in Figure 3 are the measuring and reference elements (in this application T_D and T_S respectively) [9].

Figure 3: Bridge circuit of a bolometer sensor [9]

From the circuit in Figure 3:

R_1 is the measuring element at the temperature T_D (°C) and is given by:

$$R_1 = R_0(1 + \alpha T_D) \tag{10}$$

R_2 is the reference element at the surrounding temperature T_S (°C) and is equally given by:

$$R_2 = R_0(1 + \alpha T_s) \tag{11}$$

R_0 in Equation (10) and Equation (11) is the internal resistance of the bolometer (sensor) at temperature 0 °C and α is the temperature coefficient of resistance. The two R's in the circuit are fixed value resistors. The output voltage of the bridge circuit can be approximated by:

$$V_o = V_s \left(\frac{R_o(1 + \alpha T_D)}{R + R_o(1 + \alpha T_D)} - \frac{R_o(1 + \alpha T_S)}{R + R_o(1 + \alpha T_S)} \right) \tag{12}$$

Rearranging Equation (12) yields:

$$V_o = V_s \left(\frac{1}{1 + \dfrac{R}{R_o(1 + \alpha T_D)}} - \frac{1}{1 + \dfrac{R}{R_o(1 + \alpha T_S)}} \right) \tag{13}$$

If R is chosen to be much greater than R_o (i.e $R >> R_o$) then:

$$V_o \approx V_s \left(\frac{1}{\dfrac{R}{R_o(1 + \alpha T_D)}} - \frac{1}{\dfrac{R}{R_o(1 + \alpha T_S)}} \right) \tag{14}$$

Following some simplifications, the output of the bolometer can be obtained from Equation (15).

$$V_o \approx V_s \alpha \frac{R_o}{R} (T_D - T_S) \tag{15}$$

Substituting Equation (7) in Equation (15) yields:

$$V_o \approx \frac{V_s \alpha R_o}{UAR} P_D \qquad (16)$$

In Equation (16), V_o is the output voltage (v), V_S represents the supply voltage (v), α denotes the temperature coefficient of resistance (C^{-1}), and R_o is the reference resistance (Ω).

4. RESULTS AND ANALYSIS

The authors of this paper did not have a selective body of precisely controlled temperature and know emissivity, a black body was used as the reference object of temperature measurement. However, the black body was tested as an object of unknown emissivity to simulate real measurement mode and task of the system. Additionally, a known detector data was used to facilitate the simulation of the real measurement process. The results of the system are discussed below. The given detector data are as follows: Heat transfer coefficient, U = 2 x 104 W m^{-2} ^{o}C^{-1}, detector surface area, A = 1.6 x 10^{-4} m^2, heat capacity, MC = 1.6 x10^{-2} J ^{o}C^{-1}, temperature coefficient of resistance, α = 0.004 ^{o}C^{-1}, reference resistance, R_o = 100 Ω at 0 ^{o}C.

The temperature range of the source is given as 900 ^{o}C – 1200 ^{o}C, the temperature of the surrounding environment is taken as 25 ^{o}C. The radiant energy from the process falls on the detector at a rate given by Equation (4). For the given source temperature range, the maximum and minimum incident power on the detector can be computed using the rate at which the radiant energy falls on the detector as:

$$P_{Dmax} = 50 \text{ x } 10^{-12} \text{ x } (1200+273)^4$$

$$= 50 \text{ x } 10^{-12} \text{ x } 1473^4$$

$$= 235.39 \text{ W}$$

$$P_{Dmin} = 50 \text{ x } 10^{-12} \text{ x } (900+273)^4$$

$$= 50 \text{ x } 10^{-12} \text{ x } 1173^4$$

$$= 94.66 \text{ W}$$

Similary, Equation (7) was used to obtain the corresponding T_{Dmax} and T_{Dmin} as thus:

$$T_{Dmax} = \frac{235.39}{2 \text{ } x \text{ } 10^4 \text{ } x \text{ } 1.6 \text{ } x \text{ } 10^{-4}} + 25$$

$$= 73.56 + 25$$

$$= 98.56 \text{ }^o\text{C}$$

$$T_{Dmin} = \frac{94.66}{2 \text{ } x \text{ } 10^4 \text{ } x \text{ } 1.6 \text{ } x \text{ } 10^{-4}} + 25$$

$$= 29.54 + 25$$

$$= 54.58 \text{ }^o\text{C}$$

Now, since $R \gg R_o$ and for design purposes, R can be chosen to be approximately = 10 KΩ. For the detector to be within 2% of equilibrium when the chopper (shutter) switches, the relationship below must be satisfied. i.e:

$$\tau_D < \frac{1}{6 f_c} \qquad (17)$$

where denotes the time constant of the detector (usually in ms) and f_c represents the chopping frequency of the rotating shutter. Using Equation (8), the detector time constant is computed as:

$$\tau_D = \frac{1.6 \times 10^{-2}}{2 \times 10^4 \times 1.6 \times 10^{-4}}$$

$$\tau_D = 5 \times 10^{-3} \text{s}$$

$$\tau_D = 5 \text{ ms}$$

Therefore, recall Equation (17) and substituting the value of the time constant yields:

$$5 \text{ ms} < \frac{1}{6f_c}$$

$$30 \text{ ms} < \frac{1}{f_c}$$

$$f_c < \frac{1}{30 \text{ ms}}$$

$$f_c < 33.33 \text{ Hz}$$

Therefore, choosing f_c so the above relationship is satisfied, so $f_c = 30$ Hz which effectively means that the shutter is rotating at 1800 rpm. Now, the pulse duration time for the shutter cycles is thus:

$$T_p = \frac{1}{30}$$

$$T_p = 33.33 \text{ ms}$$

This means that, since the detector has the behavior of a first order system, the detector will have enough time to settle before the next shutter transition. This is illustrated in the Figure 4 below:
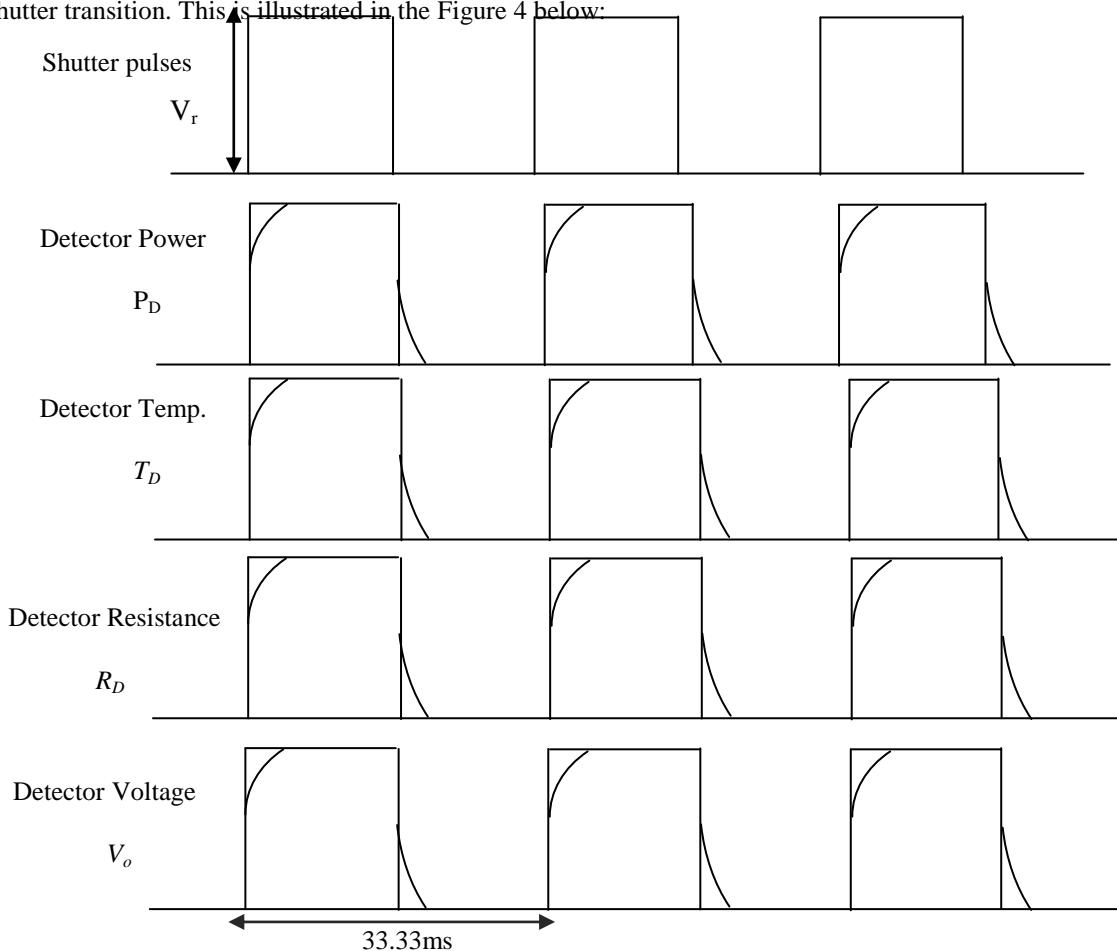
Figure 4: Shape of the shutter pulses and the detector behaviour

Figure 4 shows how the detector tries to catch up with the shutter pulses and settles before the next shutter transition.

The maximum output voltage of the detector V_{omax} occurs when P_D and T_D are maximum and this corresponds to the amplitude of the chopper (shutter) pulses. Recall Equation (15) thus:

$$V_{omax} \approx V_s \alpha \frac{R_o}{R}(T_{Dmax} - T_S) \tag{18}$$

Since the output of the detector (bridge output) is very small, as a result is going to be very susceptible to environmental noise, a PSD is used which can be regarded as a multiplier or demodulator plus a low pass filter and form the basis of a lock in amplifier. Using the PSD, the effects of noise can be substantially reduced, enabling small signals to be recovered from an extremely noisy environment. The PSD output using square wave reference signal is:

$$V_{PSD} = \frac{2VV_r}{\pi} cos\theta \tag{19}$$

where V_r denotes the amplitude of the shutter pulse $= V_{omax}$ (at maximum temp.) Now, V_{omax} from Equation(18) and substituting T_{Dmax} computed above, and $V_S = 0.707V$ (rms value):

$$V_{omax} = 0.707V \ x(0.004)\frac{100}{10000}(98.56 - 25)$$

$$V_{omax} = 2.08 \ x \ 10^{-3} \ x \ V \ (V) \tag{20}$$

Substituting V_{omax} into Equation (19) and assuming $\theta = {}^o0$ for maximum output, which should be less than or equal to 1V (ADC maximum range):

$$V_{PSD} = \frac{2 \ x \ v \ x \ 0.707v \ x2.08 \ x \ 10^{-3}}{\pi} \le 1$$

$$V^2 = \frac{\pi}{2 \ x \ 2.08 \ x \ 10^{-3}}$$

$$V^2 = 755.19$$

$$\therefore V = 27.48 \ V$$

For design purposes, assuming $V = 21.5$ v

$$\therefore \quad V_S = 0.707 \ x \ 21.5$$

$$= 15.2005 \ V$$

$$\sim = 15 \ V$$

Therefore, by Equation (20) the maximum detector voltage (bridge output) V_{omax} which corresponds to the amplitude of the shutter pulse V_r when the detector temperature is maximum.

$$V_{omax} = 2.08 \ x \ 10^{-3} \ x \ V \ (V) = V_r$$

$$= 2.08 \ x \ 10^{-3} \ x \ 21.5$$

$$= 44.13 \ mV$$

Similarly, by Equation (19) the maximum voltage output of the phase sensitive detector (PSD) is thus:

$$V_{PSDmax} = \frac{2VV_r}{\pi} cos\theta$$

$$V_{PSDmax} = \frac{2 \; x \; 21.5 \; x \; 44.13 \; x \; 10^{-3}}{\pi} \cos(0)$$

$$V_{PSDmax} = \frac{1.8976}{\pi}$$

$$V_{PSDmax} = 0.60 \text{ V}$$

This V_{PSD} is the voltage going into the ADC digitizer. Using Equation (4), Equation (7), Equation (19), and Equation (20), and substituting where applicable $V_s = 15$ V, $R = 10$ KΩ, the values of T_D, V_o (output of the bridge), P_D and V_{PSD} are computed and tabulated as shown in Table 1.

Table 1:   Design result for broadband pyrometer system

$T \; (^oC)$	$T \; (K)$	$P_D \; (W)$	$T_D \; (^oC)$	$V_o \; (mV)$	V_{PSD}
900	1173	94.659031	54.5809471	17.7486	0.2429
915	1188	99.594594	56.1233107	18.674	0.25556
930	1203	104.72069	57.725217	19.6351	0.26872
945	1218	110.04217	59.388179	20.6329	0.28237
960	1233	115.56393	61.1137288	21.6682	0.29654
975	1248	121.29094	62.9034173	22.7421	0.31124
990	1263	127.22821	64.7588147	23.8553	0.32647
1005	1278	133.38083	66.6815098	25.0089	0.34226
1020	1293	139.75395	68.6731106	26.2039	0.35861
1035	1308	146.35278	70.7352442	27.4411	0.37555
1050	1323	153.18258	72.8695564	28.7217	0.39307
1065	1338	160.24868	75.0777122	30.0466	0.4112
1080	1353	167.55647	77.3613955	31.4168	0.42996
1095	1368	175.11139	79.7223092	32.8334	0.44934
1110	1383	182.91896	82.1621752	34.2973	0.46938
1125	1398	190.98475	84.6827343	35.8096	0.49007
1140	1413	199.31439	87.2857464	37.3714	0.51145
1155	1428	207.91357	89.9729904	38.9838	0.53351
1170	1443	216.78804	92.746264	40.6478	0.55629
1185	1458	225.94363	95.6073841	42.3644	0.57978
1200	1473	235.3862	98.5581865	44.1349	0.60401

i.   **Calibration**

From Table 1, the calibration graph of the output voltage V_{PSD} versus the source temperature is depicted in Figure 5. This is done in order to interpret the output voltage of the pyrometer in terms of the temperature. The calibration of the pyrometer from experiment is necessary because the output of the pyrometer is affected considerably by losses due to the surface condition at the face of the detector, the variation of emissivity of the object with its surface temperature, and other factors.
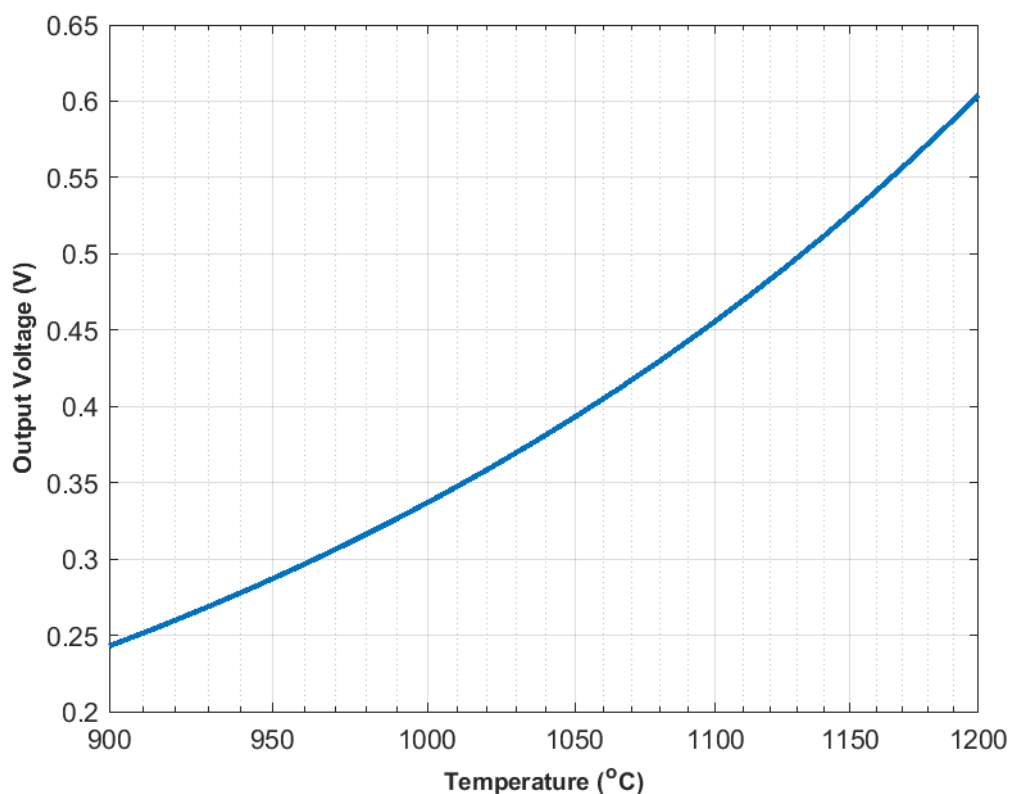
Figure 5: Calibration curve chopped broadband radiation pyrometer

However, the advantage of calibration with the black body is that high temperature accuracy measurements can be obtained with the pyrometer system. The main problem, however, is that the temperature of the black body is limited to 1200 $^{\circ}$C. The measurement of temperature higher than 1200 $^{\circ}$C is possible if theoretical calibration curve is calculated. This can be obtained using the Planck's law or Wien's law with the knowledge of the detector responses and spectral transmissions of the optical components.

Additionally, it can be seen from Figure 5 that the pyrometer temperature range configuration has approximately 0.60 V corresponding to the maximum temperature and a minimum of approximately 0.24 V corresponding to the minimum temperature in the measurement range. Furthermore, the system resolution spans in the range – 1 V to +1 V, which implies that my pyrometer configuration has limited the system to the range 0 V to 1 V as the configuration, has no negative value of voltage (i.e resolution compromised).

Interestingly, the pyrometer system accuracy based on linearity can be deduced from Equation (6) at steady state. The relationship between the incident power of the detector and the detector temperature is shown in Figure 6.
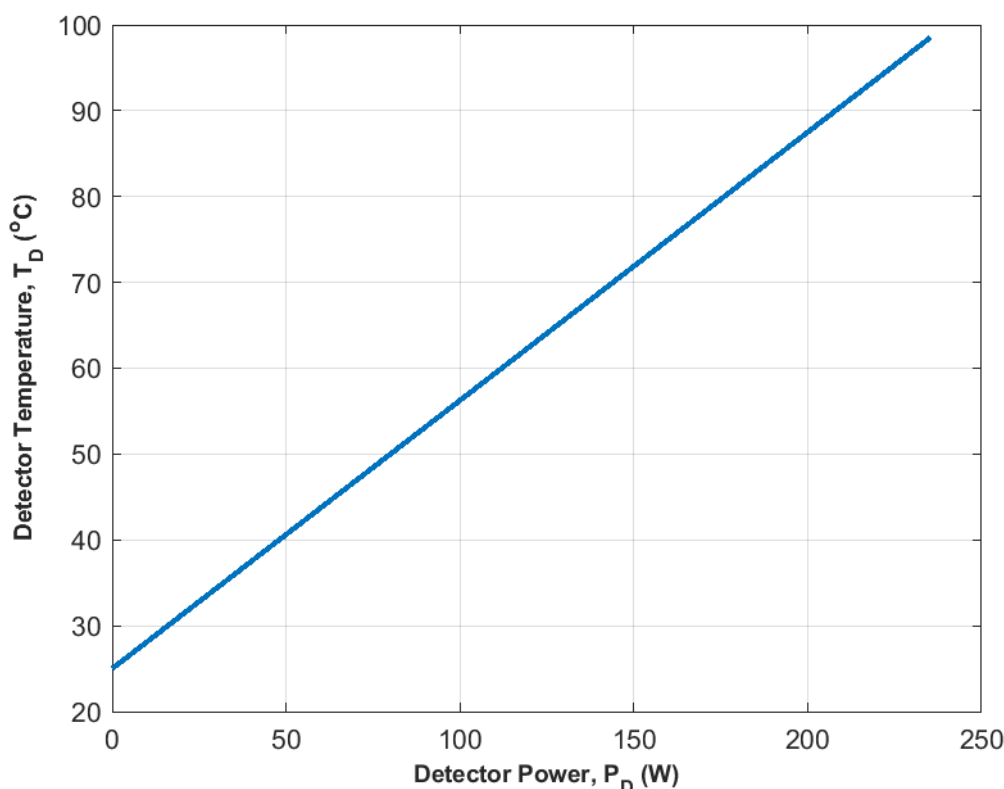
Figure 6: Linear characteristics chopped broadband pyrometer at steady state

As shown in Figure 6, the intercept on the T_D axis corresponds to the surrounding temperature T_S. Hence, a linear function $T_D = 0.3125 P_D + 25$ is obtained from the graph, where $0.3125\ (w^{-1}°C)$ is the sensitivity which corresponds to the UA relationship in Equation (7).

5. CONCLUSION

In summary, the signal conditioning and acquisition elements for a chopped broadband radiation pyrometer for temperature measurements in the range 900 ^{o}C to 1200 ^{o}C have been designed. A bolometer was used as the detector which is a passive resistive device, hence a bridge circuit was used to produce an output voltage proportional to the temperature (i.e17.75 mV to 44.13 mV) corresponding to the temperature range of the pyrometer. Since this output is very small, it implies that, is very susceptible to noise and a PSD was used in the form of lock- in amplifier plus low pass filter which amplifies, recover the signal and produce an output within the range of the digitizer (i.e 0.24 V – 0.60 V) corresponding to the temperature range. It was also shown that a suitable chopping frequency of 30 Hz was chosen for the shutter which has been verified to be within the physical properties of the system by satisfying the relationship: $\tau_D < \frac{1}{6f_c}$ in order for the detector to have enough time to settle before the next shutter transition as shown in Figure 4. Calibration graph was also provided giving the relationship of the output voltage and the temperature which is approximately linear.

REFERENCES

1. Bentley, J. P. 2005. Principles of Measurement Systems, Fourth Edition, Prentice Hall, USA. ISBN: 978 – 0 – 13043028 – 1.
2. Jack, E. K., Etu, I., and Ukanide, N. V. 2016. The Design of Signal Conditioning and Acquisition Elements of Chopped Broadband Radiation Pyrometer. *In Proceeding of the World Congress on Engineering and Computer Science*, Vol. 1.
3. Alan, M. S. 2001. Measurement and Instrumentation Principles, Third Edition, Butterworth-Heinemann, Uk.
4. Bieleck, Z. and Chrzanowski, K. 1999. Infrared Pyrometer for Temperature Measurement of Objects for both Wavelength and Time Dependent Emissivity. *Optica Applicata*, Vol. XXIX (3), Pp. 285 – 292.
5. Muller, B., and Renz, U. 2001. Development of Fast Fiber – Optic Two Color Pyrometer for the Temperature Measurement of Surfaces with Varying Emissivities. *Review of Scientific Instruments*, Vol. 72 (8), Pp. 3366 – 3374.

6. Ng, D., and Fralick, G. 2001. Use a Multiwavelength Pyrometer in Several Elevated Temperature Aerospace applications. *Review of Scientific Instruments*, Vol. 72 (1), Pp. 1522 – 1530.

7. Ueda, T., Hosokawa, A., and Yamamoto, A. 1985. Studies on Temperature of Abrasive Grains in Grinding – Application of Infrared Radiation Pyrometer. *Journal of Engineering for Industry, Transactions of the ASME*, Vol. 107, Pp. 127 – 133.

8. Vàzquez, C., Pérez-Prieto, S., López-Cardona, D. J., Tapetado, A., Blanco, E., Moreno-López, J., Montero, S. D. and Lallana, C. P. 2018. Fiber-Optic Pyrometer with Optically Powered Switch for Temperature Measurement. *Sensors*, Vol. 18 (483), Pp. 1 – 10.

9. Wallace, P. 2010. Instrumentation for Mechanical Condition Monitoring: Module Notes